*Structural Engineering and Mechanics, Vol. 4, No. 4 (1996) 437-450*
DOI: http://dx.doi.org/10.12989/sem.1996.4.4.437 

# Nonlinear finite element analysis of fibre reinforced concrete deep beams

S. Swaddiwudhipong†

*Department of Civil Engineering, The National University of Singapore, Kent Ridge, 0511 Singapore*

**Abstract.** A study on the behaviour of fibre reinforced concrete deep beams with and without web openings is carried out using nonlinear finite element analysis. Eight node isoparametric plane stress elements are employed to model the fibre reinforced concrete materials. Steel bars are treated using a compatible three node truss elements. The constitutive equations for fibre reinforced concrete materials take into account the softening effect of co-existing shear strains. Element stiffness at each step is formulated based on the tangent modulus at the current level of principal strains. Transformation between principal directions and global coordinate system is imposed. Comparison of analytical results with experimental values indicates reasonably good agreement. The proposed numerical model can be used to study the behaviour of this composite structures of practically any geometries.

**Key words:** deep beams; fibre reinforced concrete; finite element; material nonlinearity; web openings.

## 1. Introduction

Deep beams are beams with a span to depth ratio of less than about 5. Owing to their geometrical proportions, strength of deep beams is normally governed by shear rather than by flexure provided that nominal amount of longitudinal reinforcement is present. The failure mode of this type of structure is characterised by a gradual propagation of diagonal cracks towards the support and loading points along the natural load path (Kong *et al.* 1978). For deep beams with a span to depth ratio of less than 2, Chow *et al.* (1953) based on finite difference solutions showed that the distribution of stresses in such deep beams differs significantly from that of ordinary slender beams. Results from finite element analyses reaffirm the above postulate (see e.g., Fafitis and Won 1994).

When short discrete fibres are added to the concrete matrix, the fibres are able to arrest the growth of micro-cracks which will enlarge under stress to form visible cracks which ultimately cause failure. The restriction of the growth of these cracks increases the tensile strength of the concrete. Compared to steel bars, fibres are able to arrest any cracks more effectively as they are randomly distributed throughout the concrete at a much closer spacing than can be obtained by the reinforcing bars. The inclusion of these fibres also enhances the fracture toughness and post cracking ductility. The performance of the composite materials will depend on the physical and material properties of the constituents as well as the strength of the bond between the two.

† Associate Professor

Several researchers have conducted experimental investigations on the behaviour of reinforced concrete deep beams with and without steel fibres. Kong *et al.* (1970, 1978) reported results from a series of tests carried out on reinforced concrete deep beams with an without web openings. Based on these experimental results they proposed empirical formulae to predict the ultimate strength of these beams. A more rational semi-empirical formula was also presented by Ray and Reddy (1979) for the same type of structures. The behaviour of fibre reinforced concrete deep beams with and without web openings was reported by Swaddiwudhipong and Shanmugam (1985, 1994) and Shanmugam and Swaddiwudhipong (1988).

So far, no accurate theory exists for predicting the behaviour of deep reinforced concrete beams. This is due largely to the nonlinearity of the mechanical properties of the concrete materials as well as the deviation of the behaviour of deep beams from the basic beam theory. The presence of openings in this type of beams aggravates further the complexity of the problems. These openings are usually necessary to provide access to utility and service ducts without further increase in the ceiling head room.

In this paper, the finite element method is used to study the behaviour of fibre reinforced concrete deep beams. Material nonlinearity is considered in the study. Effect of shear strains on the softening of concrete materials is considered in the adopted constitutive equations. The proposed numerical model has wide application and can be used to analyse this composite structures of practically any geometries.

## 2. Constitutive models

### 2.1. Fibre reinforced concrete

It has been observed that the compressive stress of concrete is not only a function of the compressive strain but also depends on the co-existing shear strains. The shape of the compressive

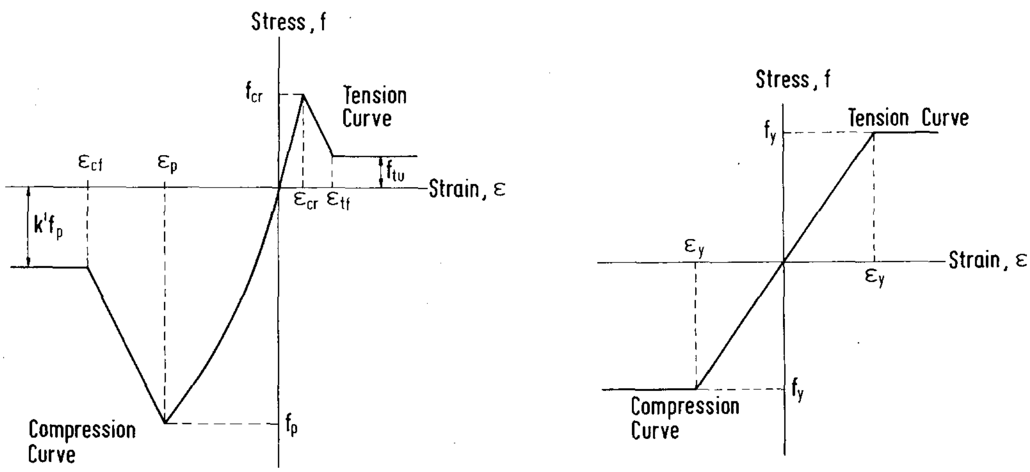


(a) (b)

Fig. 1 Stress-strain diagram of (a) concrete materials and (b) steel bar.

curve is influenced by the shear coefficient $\lambda$, which is a ratio of the shear strain to the compressive strain. Both the peak stress and the corresponding value of strain are reduced by a factor $1/\lambda$. The shear coefficient, $\lambda$, is always greater than one and reduces to unity in the case of uniaxial compression (Vecchio and Collins 1981, 1986) The stress-strain relationship of steel fibre reinforced concrete materials (Mansur and Ong 1991) is shown in Fig. 1(a). The constitutive model for each regime depends on the state of principal strains in concrete. The constitutive equations for various regimes of principal strains can be expressed as follows:

### *2.1.1. Concrete under compression*

(1) Prior to reaching strain corresponding to peak stress, $|\varepsilon_d|<|\varepsilon_p|$

$$f_d=f_c'\left[2\frac{\varepsilon_d}{\varepsilon_o}-\lambda\left(\frac{\varepsilon_d}{\varepsilon_o}\right)^2\right] \tag{1}$$

(2) Strain softening range, $|\varepsilon_p|\le|\varepsilon_d|<|\varepsilon_{cf}|$

$$f_d=f_p\left[1-\frac{\varepsilon_d-\varepsilon_p}{\varepsilon_{cf}-\varepsilon_p}(1-k)\right] \tag{2}$$

(3) Constant stress regime, $|\varepsilon_d|\ge|\varepsilon_{cf}|$

$$f_d=k'f_p \tag{3}$$

where

$$\lambda=\left(\frac{\gamma_m}{\varepsilon_d}-\nu\right)^{0.5} \tag{4a}$$

$$f_p=\frac{f_c'}{\lambda} \tag{4b}$$

$$\varepsilon_p=\frac{\varepsilon_o}{\lambda} \tag{4c}$$

$$\varepsilon_{cf}=\frac{0.041-2\varepsilon_o f_c'}{f_c'-6.896}+\varepsilon_o \tag{4d}$$

$$k=0.38V_f\frac{1_f}{\phi_f} \tag{4e}$$

The maximum shearing strain, $\gamma_m=\varepsilon_d-\varepsilon_r$; $f_c'$ is the cylindrical compressive strength in MPa; $\nu$ the Poisson's ratio of concrete; $\varepsilon_o(=0.002)$, is the strain at the maximum compressive stress of nonsoftened concrete; $V_f$ the volume fraction of steel fibre; $1_f$ the length of the fibre in mm; $\phi_f$ the equivalent diameter of the fibre in mm and $f_d$, $f_r$, $\varepsilon_d$ and $\varepsilon_r$ are the current state of principal stresses and principal strains respectively. The expression for threshold value of strain for constant stress regime Eq. (4d) was given by Kent and Park (1971) while the fibre coefficient $k$ in Eq. (4e) was obtained empirically from the test results of Fanella and Naaman (1985).

### *2.1.2. Concrete under tension*

(1) Prior to cracking in concrete, $\varepsilon_r<\varepsilon_{cr}$

$$f_r = (\varepsilon_r - 0.15\,\varepsilon_d)\,E_c \tag{5}$$

(2) Strain softening range, $\varepsilon_{cr} \leq \varepsilon_r < \varepsilon_{tf}$

$$f_r = (f_{cr} - f_{tu}) \cdot \frac{\varepsilon_r - \varepsilon_{cr}}{\varepsilon_{cr} - \varepsilon_{tf}} + f_{cr} \tag{6}$$

(3) Constant stress regime, $\varepsilon_r \geq \varepsilon_{tf}$

$$f_r = f_{tu} \tag{7}$$

where

$$\varepsilon_{tf} = 2f_y\left(\frac{1}{E_s} + \frac{\rho_t}{E_c}\right) \tag{8a}$$

$$f_{tu} = 2\eta_l\,\eta_o\,\tau_{uf}\,V_f\,\frac{l_f}{\phi_f} \tag{8b}$$

$$E_c = \frac{2f_c'}{\varepsilon_o} \tag{8c}$$

$E_s$ and $f_y$ are Young's modulus of elasticity and yield stress of steel respectively; $\rho_t$ is the reinforcement ratio, $\eta_l(=0.5)$, the length efficiency of the fibre; $\eta_o(=0.33)$, the orientation factor for the fibre and $\tau_{uf}(=4.12$ MPa), the ultimate bond strength between the fibre and concrete matrix. Eqs. (8a) and (8b) were proposed by Barzegar and Schnobrich (1988) and Lim *et al.* (1986) respectively.

### 2.2. Steel bars

The steel bars are modelled as an elastic-perfectly-plastic material as shown in Fig. 1(b). The constitutive equations of steel bars in concrete is expressed as follows:
Before yielding, $|\varepsilon| < |\varepsilon_y|$

$$f = E_s\,\varepsilon \tag{9}$$

and after yielding, $|\varepsilon| \geq |\varepsilon_y|$

$$f = f_y \tag{10}$$

## 3. Finite element solution

The finite element package "ABAQUS" is employed in the analysis. Eight-node isoparametric plane stress elements with a 3×3 Gauss point quadrature as shown in Fig. 2(a) are used to model the fibre reinforced concrete materials. The main reinforcement is treated as comprising several three-node truss elements attached to the boundary of plane stress elements at the assigned locations. The total amount of web reinforcement in each direction is evaluated, and evenly distributed as truss elements attached to the boundary of plane stress elements. The truss element with 2 Gauss point quadrature is depicted in Fig. 2(b). Perfect bond between steel bars and matrix materials is assumed. This is especially true for the main reinforcement which is fully

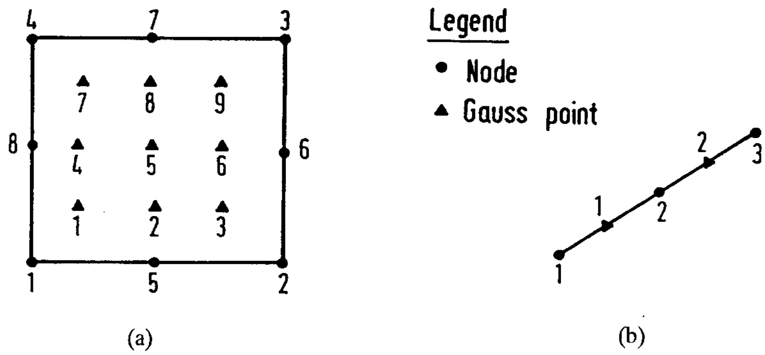


Fig. 2 Finite element model (a) eight-node plane stress element for concrete matrix and (b) three node truss element for steel bar.

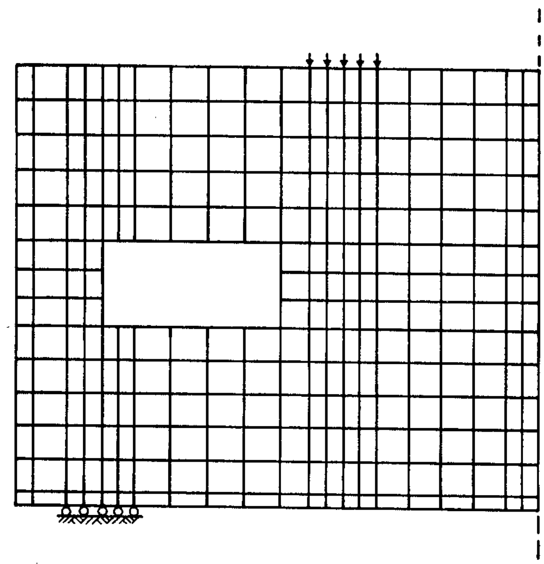

Fig. 3 Typical finite element mesh for beams with openings.

anchored to the side steel plates as described in the experimental study (Swaddiwudhipong and Shanmugam 1985, 1994). No element is present at the openings. A typical finite element mesh for beams with openings is depicted in Fig. 3.

Since the material properties of the constituents are highly nonlinear, a nonlinear solver is unavoidable. The modified Riks method (Riks 1972, Crisfield 1981 and Ramm 1981) is adopted in the solution process of the resulting nonlinear stiffness equations. Static option, assisted by automatic incrementation scheme based on displacement-controlled procedure (Hibbitt, Karlsson and Sorensen Inc. 1991) is adopted to control the increment size and consequently the rate of convergence of the solutions. Details on finite element formulation are available in standard finite element textbooks such as Zienkiewicz and Taylor (1989) whereas the solution process is described by Powell and Simon (1981), Ramm (1981) and Hibbitt, Karlson and Sorensen Inc. (1991).

## 4. Element stiffness matrix

Formulation of element stiffness in finite element procedure requires the knowledge of the material rigidity at current state of stresses or strains. The expressions for material stiffness for various states of strains in principal directions are as follows:

### 4.1. Fibre reinforced concrete under compression

(1) Prior to reaching strain corresponding to peak stress, $|\varepsilon_d| < |\varepsilon_p|$,

$$\frac{\partial f_d}{\partial \varepsilon_d} = f_c'\left[\frac{2}{\varepsilon_o} - \frac{2\lambda\varepsilon_d}{\varepsilon_o^2} - \frac{1}{2\lambda}\cdot\left(\frac{\varepsilon_r}{\varepsilon_o^2}\right)\right] \tag{11}$$

(2) During the strain softening regime $|\varepsilon_p| \leq |\varepsilon_d| < |\varepsilon_{cf}|$,

$$\frac{\partial f_d}{\partial \varepsilon_d} = \frac{f_c'(1-k')\varepsilon_r(\varepsilon_{cf}-\varepsilon_d)}{2\lambda^4\varepsilon_d^2(\varepsilon_{cf}-\varepsilon_p)}\left[1+\frac{\varepsilon_o}{(\varepsilon_{cf}-\varepsilon_p)} - \frac{2\lambda^3\varepsilon_d^2}{\varepsilon_r(\varepsilon_{cf}-\varepsilon_d)}\right] \tag{12}$$

(3) When $|\varepsilon_d| > |\varepsilon_{cf}|$,

$$\frac{\partial f_d}{\partial \varepsilon_d} = 0 \tag{13}$$

### 4.2. Fibre reinforced concrete in tension

(1) Before cracking, $\varepsilon_r < \varepsilon_{cr}$,

$$\frac{\partial f_r}{\partial \varepsilon_r} = E_c \tag{14}$$

(2) In the strain softening regime, $\varepsilon_{cr} \leq \varepsilon_r < \varepsilon_{tr}$,

$$\frac{\partial f_r}{\partial \varepsilon_r} = \frac{(f_{cr}-f_{tu})}{(\varepsilon_{cr}-\varepsilon_{tf})} \tag{15}$$

(3) When $\varepsilon_r \geq \varepsilon_{tf}$

$$\frac{\partial f_r}{\partial \varepsilon_r} = 0 \tag{16}$$

Eqs. (11)-(16) are the constitutive equations for fibre reinforced concrete materials at any state of current strains in the principal directions. In standard finite element process, the element properties are formulated in a selected global coordinate system which normally does not coincide with the principal directions. The constitutive matrix derived earlier has to be transformed to the global system prior to the application of standard finite element formulation.

The relationship between states of stresses in principal and global systems is expressed through equilibrium conditions as (Timoshenko and Goodier 1970).

$$\begin{Bmatrix} \sigma_x \\ \sigma_y \\ \tau_{xy} \end{Bmatrix} = \begin{bmatrix} \cos^2\alpha & \sin^2\alpha \\ \sin^2\alpha & \cos^2\alpha \\ \sin\alpha\cos\alpha & -\sin\alpha\cos\alpha \end{bmatrix} \begin{Bmatrix} f_r \\ f_d \end{Bmatrix} \tag{17}$$

or

$$\{\sigma\}=[T]^T\{\sigma_p\} \tag{18}$$

where $\alpha$ is the angle between the principal and global axes.

Principle of contragradient gives

$$\{\varepsilon_p\}=[T]\{\varepsilon\} \tag{19}$$

and

$$[D]=[T]^T[D_p][T] \tag{20}$$

where $[D]$ and $[D_p]$ are the element stiffness matrices in the global system and principal strain directions respectively.

## 5. Description of tested specimens

A total of eleven fibre reinforced concrete deep beams reported earlier by Singh (1990) and Swaddiwudhipong and Shanmugam (1994) are analysed using the proposed numerical models. All the beams share the same dimensions, the same clear span and are all reinforced by two 16 mm diameter bars anchored by welding to 10 mm thick steel plates at both ends. The yield strength of the bars is 408 MPa. The length, the depth and the thickness of the beams are 1550 mm, 650 mm and 80 mm respectively. Details of the beam geometry, locations and size of web openings are tabulated in Table 1 and illustrated in Figs. 4 and 5. The cube strength of fibre reinforced concrete matrix, $f_{cu}$ of each beam is included in Table 1.

One percent of steel fibre was added into the concrete mix. The steel fibre is of a mean diameter of 0.5 mm, a length of 30 mm, Young's modulus of elasticity of 205 GPa and a yield strength of 1172 MPa. In each beam of the A-series, 6 numbers of 6 mm deformed bars evenly

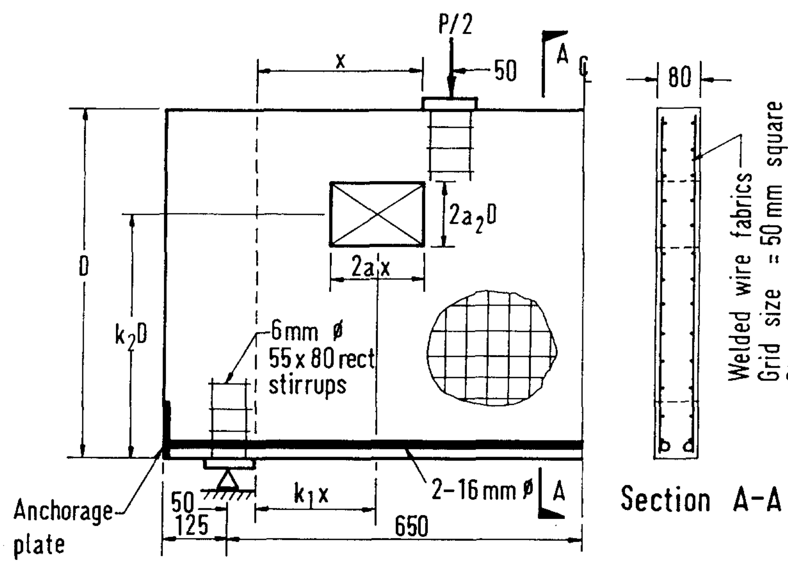


Fig. 4 Details of geometry and web reinforcement for beams of B-series.

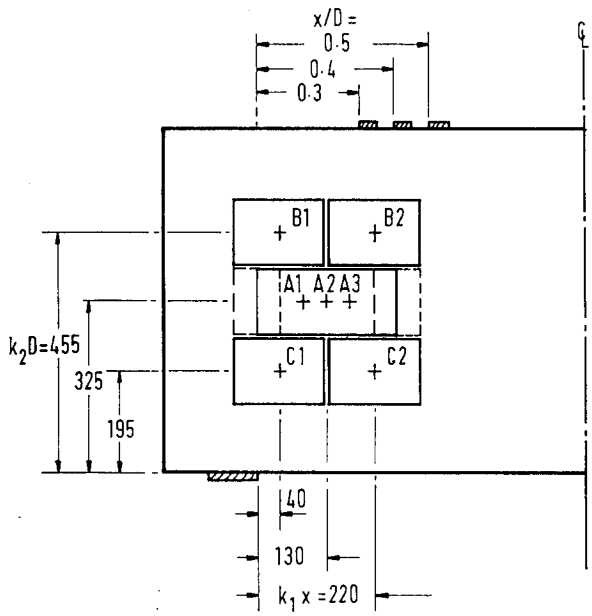


Fig. 5 Location of web openings.

Table 1 Beam geometry and concrete strength

| Series | Beam | $x/D$ | $k_1x$(mm) | $k_2D$(mm) | $2a_1x$(mm) | $2a_2D$(mm) | $f_{cu}$(MPa) |
|---|---|---|---|---|---|---|---|
| A | ASH/0.4 | 0.4 | NA | NA | NA | NA | 43.5 |
| | AOH/0.4 | 0.4 | 130 | 325 | 175 | 125 | 47.4 |
| | AOHV/0.4 | 0.4 | 130 | 325 | 175 | 125 | 43.1 |
| B | BOB1/0.3 | 0.3 | 40 | 455 | 175 | 125 | 43.3 |
| | BOC1/0.3 | 0.3 | 40 | 195 | 175 | 125 | 41.8 |
| | BOB2/0.5 | 0.5 | 220 | 455 | 175 | 125 | 41.4 |
| | BOC1/0.5 | 0.5 | 40 | 195 | 175 | 125 | 40.8 |
| | BOC2/0.5 | 0.5 | 220 | 195 | 175 | 125 | 41.1 |
| | BOA1/0.4 | 0.4 | 85 | 325 | 265 | 125 | 43.1 |
| | BOA2/0.4 | 0.4 | 130 | 325 | 265 | 125 | 43.4 |
| | BOA3/0.4 | 0.4 | 175 | 325 | 265 | 125 | 45.1 |

distributed at 100 mm c/c are provided as horizontal web reinforcement on each face. Additional 16 numbers of 6 mm bars are evenly distributed in beam AOHV/0.4 to serve as vertical web reinforcement on each face. The yield strength of web reinforcement is 446 MPa and no extra bar is provided to compensate for the reinforcement cut-out by the opening. Each beam of B-series contains on each face a layer of welded wire fabric of diameter 3.3 mm spacing at 50 mm in each direction. The yield strength of the wire employed as web reinforcement for the beams of the B-series is 304 MPa.

Each test beam was supported on a hinge at one end and on rollers at the other over a clear span of 1300 mm on a 1000 kN. Avery Universal testing machine which is a load controlled equipment. The beams were tested under two point loading symmetrically placed as shown

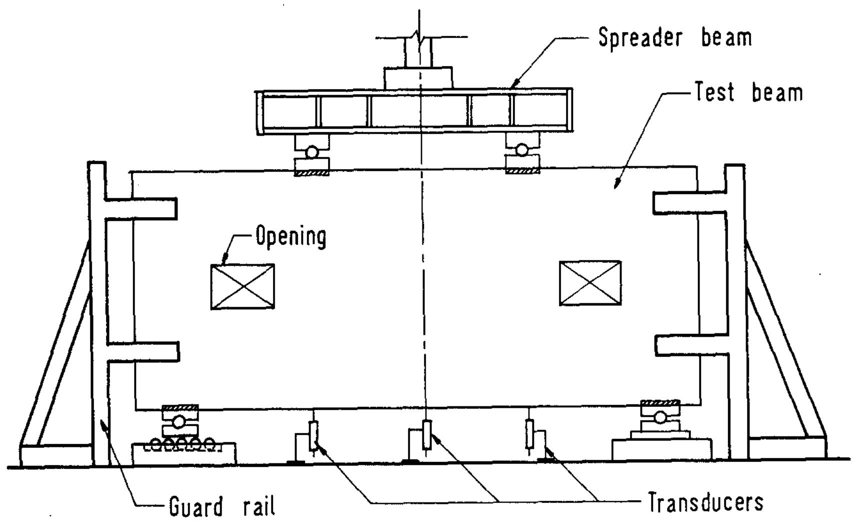


Fig. 6 Schematic diagram showing the test set-up.

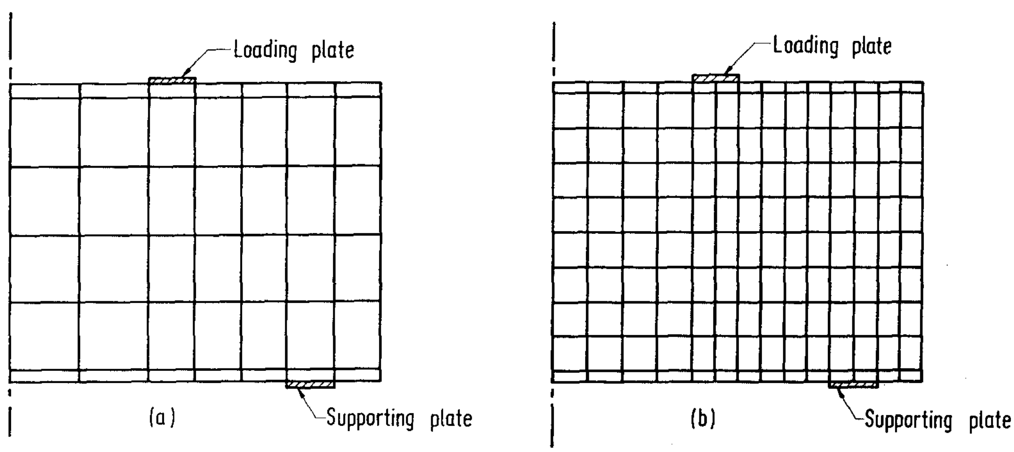


Fig. 7 Finite element meshes for beam ASH/0.4.

in Fig. 6. Loading plates were provided to prevent the crushing of concrete at the loading and supporting points. All the beams were tested to failure and vertical displacements at midspan as well as under the loading points were monitored. Details of the testing procedure can be found from Swaddiwudhipong and Shanmugam (1994).

## 6. Results and discussions

Owing to the symmetrical condition about the vertical axis at the centre of each beam, only half of the beam is considered in the analysis. Symmetrical boundary conditions are imposed along the line of symmetry. Loads are assumed acting uniformly under the loading plate and the vertical displacements of the lower nodes at the elements in full contact with the supporting

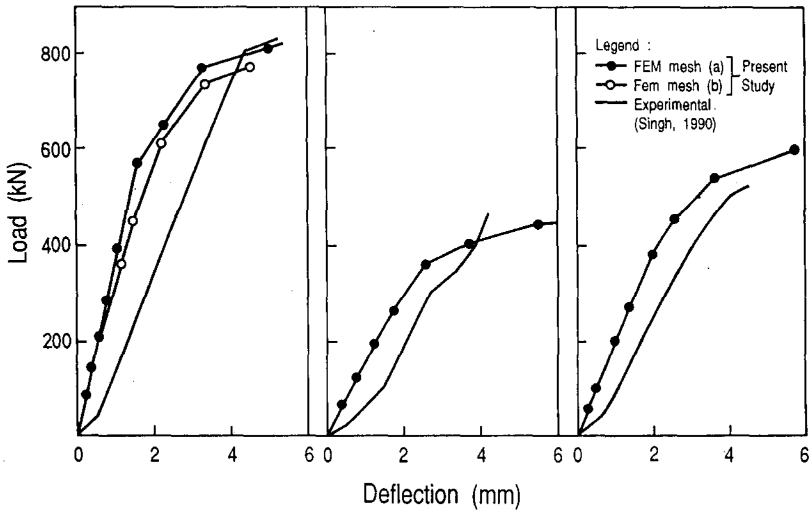


Fig. 8 Load-deflection curve of beams (a) ASH/0.4, (b) AOH/0.4 and (c) AOHV/0.4.

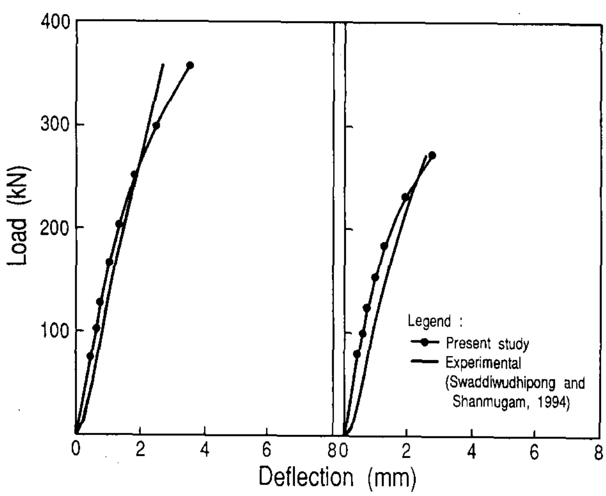


Fig. 9 Load-deflection curve of beams (a) BOB1/0.3 and (b) BOC1/0.3.

plate are constrained.

Convergence study was carried out for beams with and without openings to establish the appropriate mesh size. As an example, the results from the analyses of beam ASH/0.4 based on 2 mesh sizes shown in Fig. 7 are given in Fig. 8(a) along with those obtained from experimental investigation. The values from the two finite element analyses show close agreement implying sufficiently refined mesh size. Finite element and experimental load-deflection curves of each beam are depicted in Figs. 8-11. Numerical results deviate somewhat from the raw experimental data. However, if slackening in the early part of the test results is corrected, analytical and experimental values agree reasonably well.

The load carrying capacities of each beam obtained (1) experimentally, (2) through a semi-empirical modified Kong and Sharp formula (Swaddiwudhipong and Shanmugam 1994) and

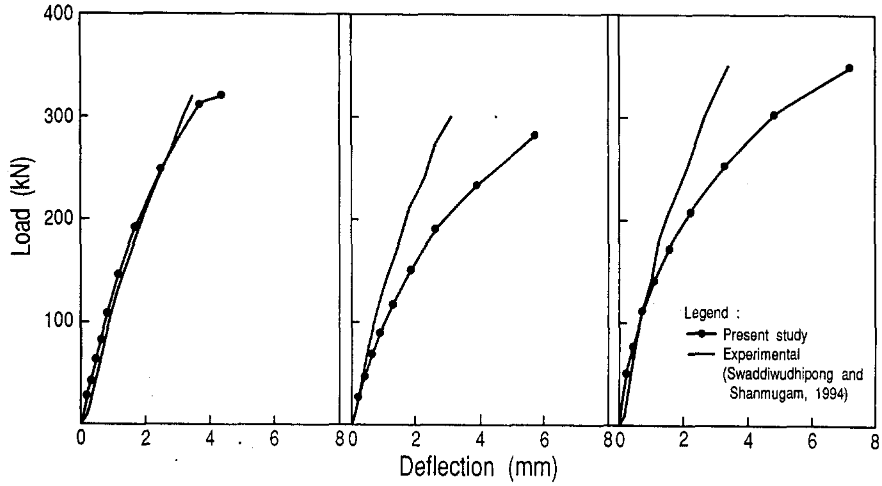


Fig. 10 Load-deflection curve of beams (a) BOA1/0.4, (b) BOA2/0.4 and (c) BOA3/0.4.

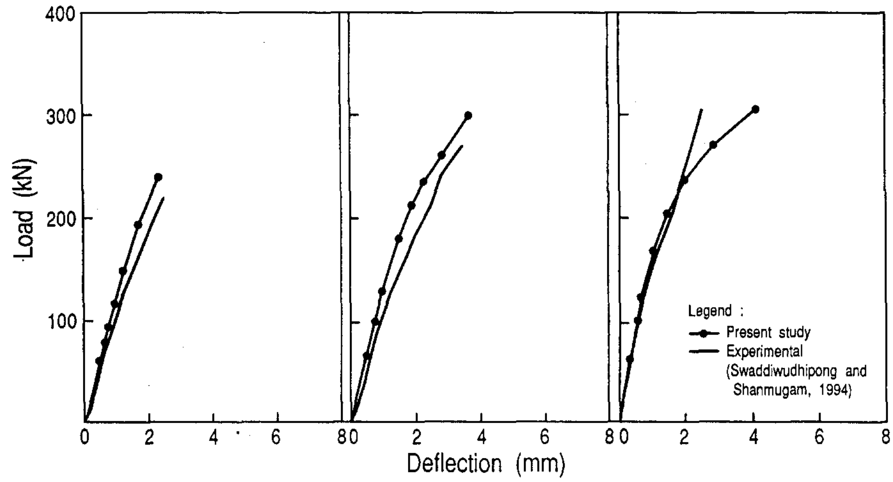


Fig. 11 Load-deflection curve of beams (a) BOB2/0.5, (b) BOC1/0.5 and (c) BOC2/0.5.

(3) finite element solutions are tabulated in Table 2. All finite element solutions but one overpredict the ultimate load when compared with experimental values. This is most likely due to (1) the assumption that perfect bond between web reinforcement and matrix materials exist and (2) local defects in the test beam which propagate when the applied load is close to the ultimate load causing the beam to fail earlier than predicted. In all study cases, the finite element values deviate within 20% from experimental results. Finite element solutions also agree reasonably well with those obtained from the modified Kong and Sharp formula. Larger discrepancies between the latter two solutions for beams AOHV/0.4 and BOB2/0.5 are noted and this is most likely due to the semi-empirical nature of the modified Kong and Sharp formula where certain coefficients were established from linear regression analysis based on experimental results.

As expected, the ultimate strength of deep beams depend largely on the presence of web

Table 2 Comparison of ultimate strength of deep beams

| Ref | Beam | FEM $P_{FEM}$(kN) | Experimental $P_{exp}$(kN) | Modified Kong & Sharp Formula $P_{MKS}$(kN) | $\frac{P_{FEM}}{P_{exp}}$ | $\frac{P_{FEM}}{P_{MKS}}$ |
|---|---|---|---|---|---|---|
| Singh (1990) | ASH/0.4 | 850 | 854 | 838 | 1.00 | 1.01 |
| | AOH/0.4 | 480 | 458 | 471 | 1.05 | 1.02 |
| | AOHV/0.4 | 595 | 520 | 489 | 1.14 | 1.22 |
| Swaddiwudhipong & Shanmugam (1994) | BOB1/0.3 | 499 | 495 | 461 | 1.01 | 1.08 |
| | BOC1/0.3 | 356 | 310 | 325 | 1.15 | 1.10 |
| | BOB2/0.5 | 416 | 350 | 321 | 1.19 | 1.30 |
| | BOC1/0.5 | 329 | 280 | 274 | 1.18 | 1.20 |
| | BOC2/0.5 | 454 | 480 | 429 | 0.95 | 1.06 |
| | BOA1/0.4 | 457 | 397 | 386 | 1.15 | 1.18 |
| | BOA2/0.4 | 356 | 340 | 364 | 1.05 | 0.98 |
| | VOA3/0.4 | 470 | 400 | 395 | 1.17 | 1.19 |

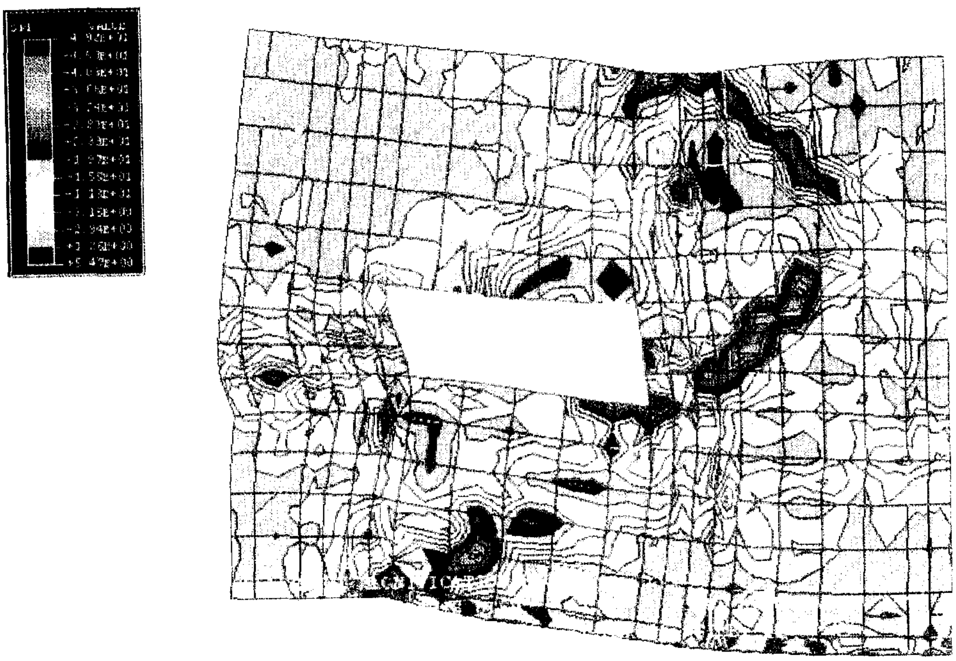

Fig. 12 Typical display showing principal stress distribution.

openings and the extent to which these openings interrupt the load path. The introduction of web openings in solid beam ASH/0.4 forming beam AOH/0.4 reduces the load carrying capacity from 850 kN to 480 kN. The beams with openings that intercept the load path to a greater extent show substantial reduction of ultimate strength. The ultimate strength of beam BOB1/0.3 as compared to beam BOC1/0.3 decreases from 499 kN to 356 kN. The openings in beam BOC1/0.3 obviously intercept to a greater extent the load path than those of beam BOB1/0.3. Another example is the comparison of ultimate load of beam BOA2/0.4 with those of beams BOA1/0.4 and BOA3/0.4. The load carrying capacity of beam BOA2/0.4 is 356 kN which is significantly lower than the valus of 457 kN and 470 kN for beams BOA1/0.4 and BOA3/0.4 respectively. The openings in beam BOA2/0.4 obviously intercept the load path more completely than those of beams BOA1/0.4 and BOA3/0.4.

The study also reveals that the ultimate strength of beams with openings in the lower portion are lower than those with openings in the higher portion when the degree of interruption of the load path is comparable. This is demonstrated through the comparison of the results of beams BOC1/0.5 and BOB2/0.5. The ultimate strength of the former is 329 kN which is substantially lower than the value of 416 kN for the latter.

A typical graphical display showing the principal stress distribution for beam with web openings is illustrated in Fig. 12. It is observed that large compressive stresses exist in the vicinity of the loading and supporting points. Tensile stresses occurs predominantly at the bottom of the beam and near the opening. The materials at the top-left corner are relatively stress free. Fig. 12 shows distinctively the flow of compressive stresses along the natural load path between the loading and supporting points around the web openings as well as thrusting each other across the symmetrical line at the level just above the top of the openings.

The study indicates that openings in deep beams, if unavoidable, should be located away from the load path i.e., in the region where stresses are relatively low. The ideal place for the problem under study will be in the vicinity of the top corner above the support or in the lower part of the beam somewhere below the loading point and midspan preferably at about middepth closer to the midspan. The amount of reinforcement loss due to the cut-out for the openings should be approximately doubled and provided around the openings. It is a good measure to provide diagonal steel bars with sufficient anchorage length at the four corners of the penings especially those lie in the vicinity of the load path.

## 7. Conclusions

The behaviour of fibre reinforced concrete deep beams with and without web openings is studied using finite element method. Effect of shear strains on the principal compressive strains as well as nonlinearity of concrete materials are considered. Finite element solutions compare reasonably well with experimental results especially when inherent error in the latter is eliminated. The results from the study reinforce the postulate that ultimate strength of deep beams depends largely on the presence, the locations of web openings and be affected significantly by the extent to which these openings interrupt the load path. Openings, if required, should be located in the low compressive stress zone. The model as proposed herein can be empolyed to study the effect of size and locations of openings on the behaviour of fibre reinforced concrete deep beams of practically any geometries.

## Acknowledgements

The contributions of Ms. L.L. Tan and Mr. V.V. Srihari on computational work are appreciated.

## References


Barzegar, F. and Schnobrich, W.C. (1988), "Modelling tension stiffening in finite element analysis of R.C. panels", *Proceedings, Canadian J. Soc. for Civ. Engrg.* **3**, 277-303.

Chow, L., Conway, H.D. and Winter, G. (1953), "Stresses in deep beams", *Transactions ASCE,* **118**(2557), 686-708

Crisfield, M.A. (1981), "A fast incremental/iteration solution procedure that handles snapthrough", *Computers and Structures,* **13**, 55-62.

Fafitis, A. and Won, V.H. (1994), "Nonlinear finite element analysis of concrete deep beams", *Journal of Structural Engineering, ASCE,* **120**, 1202-1220.

Fanella, D.A. and Naaman, A.E. (1985), "Stress-strain properties of fibre reinforced mortar in compression", *ACI J. Proceedings,* **82**, 475-483.

Hibbitt, Karlsson, and Sorensen Inc. (1991), *ABAQUS Manual,* **1**: *User's Manual,* **3**: *Example Problem Manual,* Providence, R.I.

Kent, D.C. and Park, R. (1971), "Flexural members with confined concrete", *ASCE Proceedings*, **97**, ST 7, 1969-1990.

Kong, F.K. and Robins, P.J. (1970), "Web reinforcement effects on deep beams", *ACI Journal, Proceedings*, **67**, 1010-1017.

Kong, F.K., Sharp, G.R., Appleton, S.C., Beaumont, C.J. and Kubik, L.A. (1978), "Structural idealization of deep beams with web openings: further evidence", *Magazine of Concrete Research*, **30**, 89-95.

Lim, T.Y., Paramasivam, P., Mansur, M.A. and Lee, S.L. (1986), "Tensile behaviour of steel fibre reinforced cement composites", *Proceedings 3rd RILEM Int. Sym. on Developments in Fibre Reinforced Cement and Concrete,* U.K., 7-16.

Mansur, M.A. and Ong, K.C.G. (1991), "Behaviour of reinforced fibre concrete deep beams in shear", *ACI Structural Journal*, **88**, 98-105.

Powell, G. and Simon, J. (1981), "Improved iteration strategy for nonlinear structures", *International Journal for Numerical Methods in Engineering*, **17**, 1455-1467.

Ramm, E. (1981), "Strategies for tracing the nonlinear response near limit points", *Nonlinear Finite Element Analysis in Structural Mechanics*, Wunderlich, W., Stein, E. and Bathe, K.J., Springer-Verlag, Berlin.

Ray, S.P. and Reddy, C.S. (1979), "Strength of reinforced concrete deep beams with and without opening in the web", *The Indian Concrete Journal*, **53**, 242-246.

Riks, E. (1972), "The application of Newton's method to the problem of elastic stability", *Journal Applied Mechnics*, **39**, 1060-1066.

Shanmugam, N.E. and Swaddiwudhipong, S. (1988), "Strength of the fibre reinforced concrete deep beams containing openings", *International Journal of Cement Composites and Lightweight Concrete,* **10**, 53-60.

Singh, H. (1990), "Fibre reinforced concrete deep beams with openings", *Thesis Research Project*, the National University of Singapore, Singapore.

Swaddiwudhipong, S. and Shanmugam, N.E. (1985), "Fibre reinforced concrete deep beams with openings", *Journal of the Structural Engineering, ASCE*, **111**, 1679-1690.

Swaddiwudhipong, S. and Shanmugam, N.E. (1994), "Experimental study of fibre-reinforced concrete deep beams containing openings", *The Indian Concrete Journal,* **68**, 367-372.

Timoshenko, S.P. and Goodier, J.N. (1970), *Theory of elasticity, 3 Ed.,* McGraw Hill Book Co., New York.

Vecchio, F.J. and Collins, M.P. (1981), "Stress-strain characteristics of reinforced concrete in pure shear", *Final Report, IABSE Colloquium on Advanced Mechanics on Reinforced Concrete*, Delft, 211-255.

Vecchio, F.J. and Collins, M.P. (1986), "The modified compression field theory for reinforced concrete elements subjected to shear", *ACI Journal, Proceedings,* **83**, 219-231.

Zienkiewicz, O.C. and Taylor, R.L. (1989), *The Finite Element Method*, McGraw-Hill, London.